Available online at www.sciencedirect.com
ScienceDirect
Polymer 48 (2007) 7193–7200
polymer
www.elsevier.com/locate/polymer

Preparation and crystalline morphology of biodegradable starch/clay nanocomposites

Qing-Xin Zhang [a,b,*], Zhong-Zhen Yu [c], Xiao-Lin Xie [d], Kimiyoshi Naito [b], Yutaka Kagawa [a,b]

[a] Research Center for Advanced Science and Technology (RCAST), The University of Tokyo, Tokyo 153-8505, Japan
[b] Composite Materials Group, Composites and Coatings Center (C&C), National Institute for Materials Science (NIMS), Tsukuba, 305-0047, Japan
[c] Centre for Advanced Materials Technology (CAMT), School of Aerospace, Mechanical and Mechatronic Engineering, J07, The University of Sydney, NSW 2006, Australia
[d] Department of Chemistry, Huazhong University of Science & Technology, Wuhan, China

Received 18 December 2006; received in revised form 29 August 2007; accepted 30 September 2007
Available online 6 October 2007

Abstract

An organically modified clay (o-clay) and a pristine clay (p-clay) were used to prepare biodegradable thermoplastic starch (TPS)/clay nanocomposites by melt processing. The gelatinization behaviour of starch with glycerol/H_2O was investigated and the gelatinized temperature (T_{gel}) was determined using a polarized optical microscopy (POM) equipped with a hot stage. The morphologies of gelatinized starch and extruded starch were revealed by scanning electron microscopy (SEM). Thermal stabilities of starch/clay nanocomposites were evaluated under N_2 atmosphere using thermogravimetric analysis (TGA). Transparent films of starch/clay hybrids were fabricated by hot pressing. Intercalation of starch into clay galleries and crystalline structure of starch were investigated using X-ray diffraction (XRD). It was found that the increase in *d*-spacing of organically modified clay was due to starch molecular intercalation while the increase in *d*-spacing of pristine clay was mostly caused by glycerol intercalation because of the narrow valid *d*-spacing of pristine clay and special ring-like monomer of starch. The mechanism of starch intercalation in clay galleries was discussed.

Keywords: Starch; Clay; Morphology

1. Introduction

In recent years, the environmental pollution from consumed polymers has become serious, particularly from packaging materials and one-off plastic bags and cups. Application of biodegradable polymers instead of non-biodegradable polymers is one promising way to solve the environment pollution problems caused by polymer wastes. Growing environmental concerns have created an urgent need to develop biodegradable materials that have comparable properties with today's polymeric materials at an equivalent cost. Research has been underway on producing biodegradable polymeric materials such as polycaprolactone (PCL) and poly(lactic acid) (PLA) [1–4]. However, the significant drawback, high cost, has greatly limited their wide applications. Thus, it is unlikely that they will replace the conventional non-biodegradable polymers in applications in which large quantities of materials are deployed.

Natural biopolymers have advantage over synthetic biodegradable polymers in that they are biodegradable and renewable raw materials. Starch, one of the natural biodegradable polymers, is suitable for the production of biopolymers and has been considered as one of the most promising candidates primarily because of its attractive combination of availability and price. Nearly 50% of the starch has been used for non-food applications and about 30% of the starch production is industrially precipitated from aqueous solutions because of its good film-forming properties [5]. However, starch-based materials have some drawbacks including poor mechanical

* Corresponding author. Research Center for Advanced Science and Technology (RCAST), the University of Tokyo, Tokyo 153-8505, Japan.
E-mail address: zhangqingx@gmail.com (Q.-X. Zhang).

0032-3861/$ - see front matter © 2007 Elsevier Ltd. All rights reserved.
doi:10.1016/j.polymer.2007.09.051

properties, high moisture sensitivity, and release of small molecular plasticizer from starch matrix.

There is currently a great interest in polymer–clay nanocomposites inspired by the pioneering work by researchers at Toyota which has demonstrated an improvement in both physical and mechanical properties [6,7]. Clay consists of nano layers with thickness around 1 nm and platelet aspect ratio of about 1000. Incorporation of clay may increase the mechanical properties of starch, improve the moisture resistance, and reduce the release of plasticizer from starch. Research on biodegradable starch/clay nanocomposites has been a focus in recent years. Ha et al. firstly prepared starch/clay nanocomposites by melt compounding [8,9], and it was found that clays could effectively reinforce starch-based materials and improve the thermal and barrier properties [8–15]. However, very limited reports are available on the morphology and crystalline structure of biodegradable starch/clay nanocomposites. In this study, biodegradable starch/clay nanocomposites were prepared by melt compounding. The thermal stability and crystalline morphology of starch/clay nanocomposites were investigated using TGA, SEM and XRD, and starch intercalation in clay galleries was discussed.

2. Experimental section

2.1. Materials

Native corn starch (HYLON VII) was obtained from National Starch and Chemical Company with approximately 70% amylose. Pristine clay (p-clay) and Cloisite 93A an organically modified clay (o-clay) were provided by Southern Clay Co. Glycerol (99.9%) was from Aldrich.

2.2. Gelatinization of starch

A LEITZ DMRXE polarized optical microscopy (POM) equipped with a hot stage was employed to investigate the morphology of starch granules and determine the gelatinization temperature (T_{gel}) of starch. Firstly, 5 g starch was mixed with 5 g water and 3 g glycerol, and then a drop of starch suspension was put on a glass slide and heated in the hot stage with a heating rate of 2 °C/min. The morphology of starch granules was recorded with a digital video camera. The temperature where the birefringence of the starch granules began to disappear was determined as the T_{gel} of starch.

2.3. Preparation of starch/clay nanocomposites

H_2O (500 g) and 300 g glycerol were blended for 5 min, and then 25 g clays were added into the glycerol solution and stirred seriously for 30 min at 80 °C. After the clay suspension cooled down to room temperature, 475 g native starch was added and blended for 30 min, and then gelatinized at 110 °C over night to form thermoplastic starch (TPS). The blend of TPS and clay was dried in an oven, cut into small blocks and melt extruded in a co-rotating Werner and Pfleider ZSK-30 twin screw extruder at 160 °C and a screw rotation rate of 200 rpm. Finally, the starch extrudes with about 3 wt% clay were sandwiched in PTFE films and hot pressed at 180 °C for 5 min to form films. The obtained films with the thickness of 0.5 mm were placed at room temperature for at least 48 h prior to all tests.

2.4. SEM

Starch morphology was observed using a Philips 505 scanning electron microscope with the accelerating voltage of 20 kV. All specimens were coated with gold before SEM observation. Starch specimens were broken in liquid N_2 and coated with gold prior to SEM observation.

2.5. XRD

A Siemens D5000 X-ray Diffractometer with Cu Kα radiation ($\lambda = 0.15406$ nm) at a generator voltage of 40 kV and a current of 30 mA was used. Gelatinized starch blends cut into small blocks were used for XRD, while hot pressed films of starch extrudes including TPS, TPS/p-clay and TPS/o-clay composites were used for XRD. Clay and starch powders were used directly for XRD. All experiments were carried out at ambient temperature with a scanning speed of 0.02°/s and step size of 0.02°.

2.6. TGA

TGA tests were performed from 20–450 °C at a heating rate of 20 °C/min under N_2 flow using a 2950 Thermogravimetric analyzer (TA instruments). All the specimens were dried at 40 °C for 12 h prior to TGA tests.

3. Results and discussion

3.1. Starch gelatinization and morphology

The starch used in this study is composed of two types of α-glucan, 70% amylose and 30% amylopectin. Fig. 1 shows the SEM and POM micrographies of starch granules. As seen, most of starch granules are spherulitic with size of about 10 μm, but a few rodlike granules are also observed. When viewed under polarizing microscope, numerous circular, birefringent entities exhibiting a Maltese cross are observed as shown in Fig. 1(b) which is the characteristic of crystalline structure of starch. The size of starch spherulites determined by POM agrees well with the SEM micrography, and the spherulites obtained are for positive birefringent implying that the main axes of the polymer chain are oriented in a radial direction. Starch granules are synthesized in a broad array of plant tissues, and generally exhibit positive birefringence since the refractive index is the largest along the chain axis. Variations in granule size, shape and composition depend on the botanical origin of starch [16].

It is well-known that native starch without modification cannot be melt processed directly. Starch undergoes a number

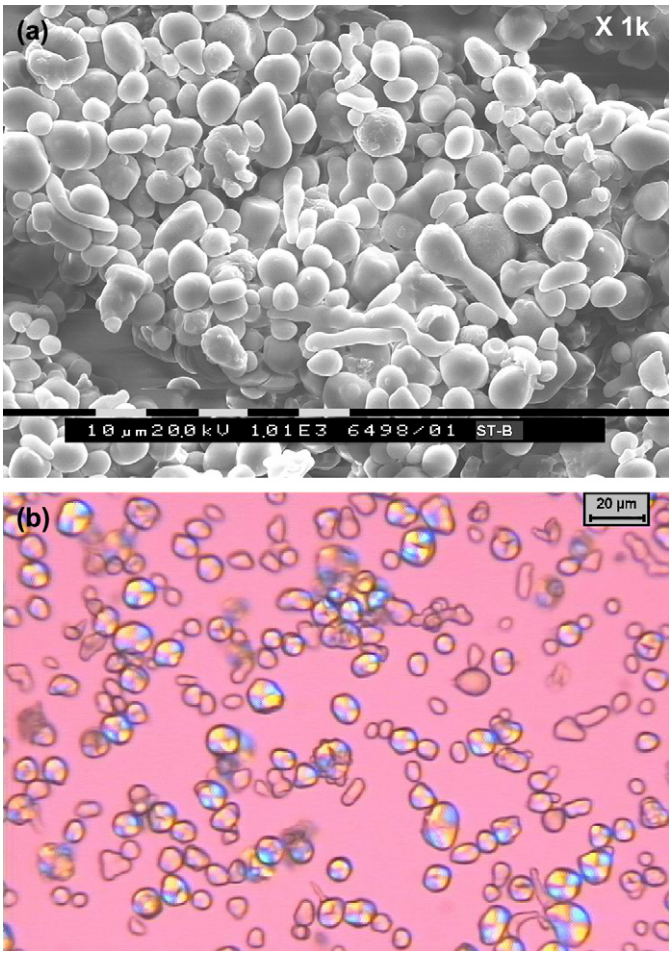

Fig. 1. Morphology of native starch: SEM (a) and POM (b).

of irreversible changes commonly referred to as gelatinization when heated in presence of a plasticizer. Starch gelatinization is primarily necessary to render starch thermoplasticity prior to melt compounding and avoid thermal decomposition during processing because its melting temperature is higher than the thermal decomposition temperature. Fig. 2 presents the gelatinization process of starch with glycerol under POM at a heating rate of 2 °C/min. Starch granules show birefringence cross clearly at 20 °C as denoted by arrows [Fig. 2(a)], and the birefringence begins to blur at 100 °C with increase in temperature [Fig. 2(b)]. Finally the birefringence of starch granules disappears completely at 110 °C [Fig. 2(c)] but it should be noticed that the shape of starch granules is kept after gelatinization. Thus, the gelatinization temperature (T_{gel}) is determined to be 100 °C which is much higher than that of some other starches which are around 70–80 °C [17]. The reason is that the starch used in this study contains more than twice as much amylose as regular corn starch which results in more rigid gels through hydrogen bonds [18].

Fig. 3 gives the SEM micrographs of gelatinized and extruded TPS, TPS/p-clay and TPS/o-clay nanocomposites. Starch granules are swelled with plasticizer, and the boundary among them nearly disappears after gelatinization. Both TPS/p-clay and TPS/o-clay nanocomposites show continuous

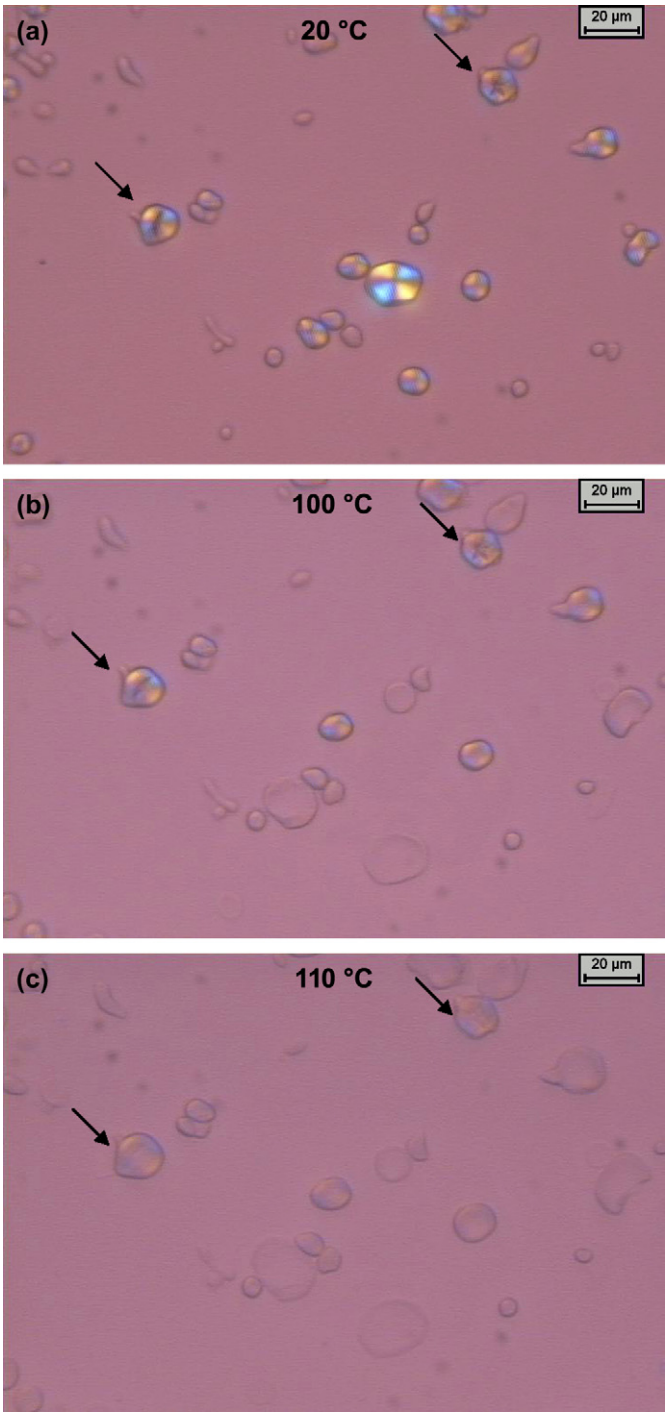

Fig. 2. POM micrographs of starch during gelatinization with glycerol at 20 °C (a), 100 °C (b), 110 °C (c).

matrix texture similar to the TPS after melt extrusion which is favourable to fabricate starch films/sheets for coating and packing applications. The obtained starch/clay films with thickness of about 0.5 mm are shown in Fig. 4. As seen, all the films are homogeneous and transparent as indicated by the fact that the words under the film can be seen clearly indicating the starch films possess low degree of crystallinity and the clays, including both pristine clay and organically modified clay, disperse homogeneously in starch matrix.

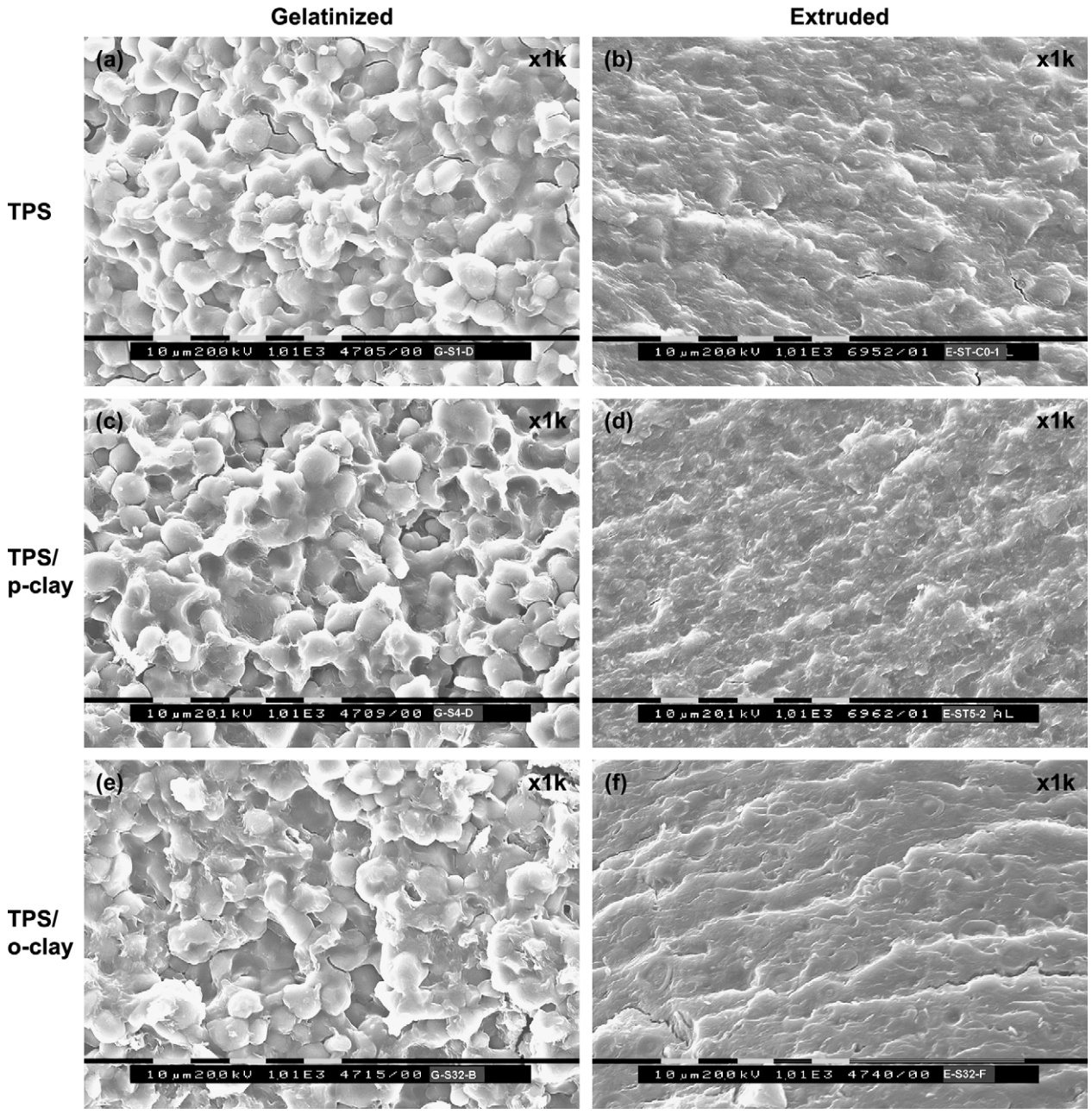

Fig. 3. SEM micrographs of gelatinized TPS (a), extruded TPS (b), TPS/p-clay (c), TPS/p-clay (d), TPS/o-clay (e) and TPS/o-clay (f).

However, there are still some differences among them. With the incorporation of pristine clay, the colour of starch film becomes much deeper, from light yellow of TPS to brown of TPS/p-clay, whereas the TPS/o-clay film shows light yellow colour ascribing to the better dispersion of o-clay in starch. Obviously, the homogeneous and transparent characters of the starch films are advantages for application as packing materials.

3.2. Thermal stability

TGA was performed to examine the thermal stability of extruded TPS, TPS/p-clay and TPS/o-clay nanocomposites, and their TGA and DTG (derivative thermogravimetry) curves are shown in Fig. 5. The initial decomposition temperatures ($T_{d\ ini}$) and the maximum decomposition temperatures ($T_{d\ max}$) are, respectively, determined from the temperature at which 5% decomposition occurs, and the peak of DTG curve. The results of $T_{d\ ini}$ and $T_{d\ max}$ are summarized in Table 1. As can be seen, both the pristine clay and the organically modified clay improve the initial decomposition temperatures of TPS. The TPS/p-clay nanocomposite exhibits a maximum decomposition temperature at 349 °C which is higher than that of TPS (344 °C), however, the $T_{d\ max}$ of TPS/o-clay nanocomposite decreases to 335 °C which might be ascribed to the decomposition of the organic alkyl ammonium used to modify clay as most alkyl ammonium modifiers starts to decompose above 200 °C [19].

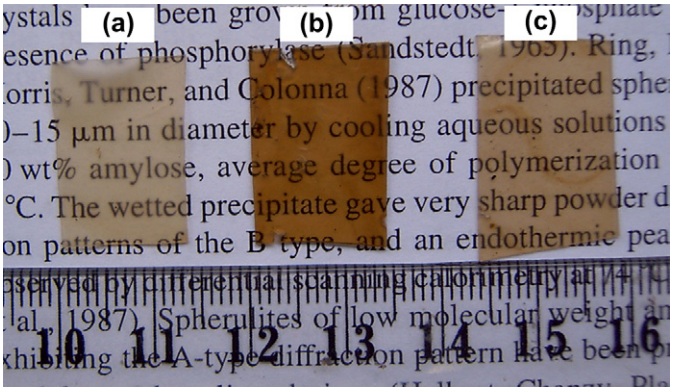

Fig. 4. Hot pressed starch films: TPS (a), TPS/pristine clay (b), and TPS/organically modified clay nanocomposites (c).

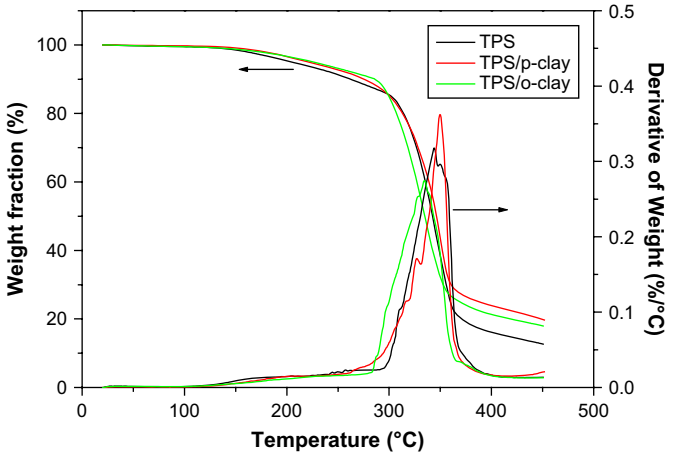

Fig. 5. TGA and DTA curves of TPS, TPS/p-clay and TPS/o-clay nanocomposites.

3.3. Crystalline structure

Native starches generally exhibit two main crystalline types, namely, the A-type for cereal starches and the B-type for tuber and amylose-rich starches [16]. The characteristic difference between their XRDs is that B-type has a strong diffraction at $2\theta = 5.5^\circ$ [20,21]. The XRDs of native starch, TPS, TPS/p-clay, and TPS/o-clay nanocomposites are shown in Figs. 6–8, respectively. Multi-peak fitting was performed to get the integrated area of crystalline peaks and amorphous peak, and the degree of crystallinity [X_c (%)] was determined by

$$X_c(\%) = \frac{A_c}{A_c + A_a} \times 100\% \quad (1)$$

where A_c is integrated area of crystalline peaks and A_a is integrated area of amorphous peak. The native starch shows a degree of crystallinity of 26% and it decreases to nearly half after gelatinization indicating the destroying of crystalline starch granules during gelatinization. The native starch shows the typical B-type structure with the space group $P6_1$ in a hexagonal unit cell ($a = b = 1.85$ nm, $c = 1.04$ nm) [21]. After extruding with glycerol, a significant change in XRD patterns is observed as demonstrated in Fig. 6 and starches transform into Va-type structure ($a = 1.30$, $b = 2.25$ and $c = 0.79$ nm, space group $P2_12_12_1$, [21]) from B-type with much sharper diffraction peaks indicating larger crystallite size formed in TPS ascribing to the introduction of glycerol which increases

Table 1
TGA and XRD parameters of starches

Material	$T_{d\text{ini}}$ (°C)	$T_{d\text{max}}$ (°C)	2θ (°)	*hkl*	*d*-Spacing (Å)	Intensity[a]	Crystalline type	X_c (%)
Native starch	–	–	5.7	100	15.5	m	B-type	26
			15.0	120	5.9	m		
			17.1	030	5.2	vs		
			20.0	130	4.4	s		
			22.4	131	4.0	m		
			23.9	302	3.7	m		
			26.2	231	3.4	w		
TPS	205	344	13.6	111	6.5	s	Va-type	13
			16.1	220	5.5	m		
			19.1	221	4.6	m		
			20.9	310	4.2	vs		
			26.3	132	3.4	w		
			29.5	232	3.0	vs		
TPS/p-clay	221	349	13.6	111	6.5	s	Va-type	10
			19.8	221	4.5	m		
			20.9	310	4.2	vs		
			25.1	122	3.5	m		
			29.5	232	3.0	vs		
TPS/o-clay	226	335	13.6	111	6.5	vs	Va-type	11
			16.5	220	5.4	m		
			19.4	221	4.6	m		
			20.9	310	4.2	vs		
			29.4	232	3.0	vs		

[a] s = Strong; m = medium; w = weak; v = very.

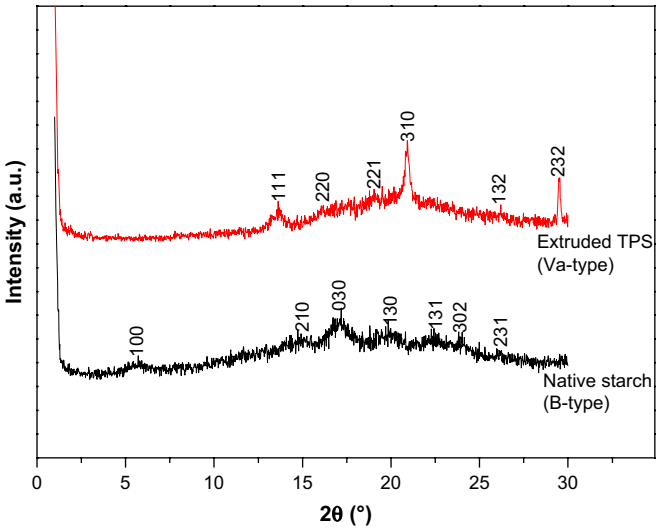

Fig. 6. XRDs of native starch and extruded thermoplastic starch (TPS).

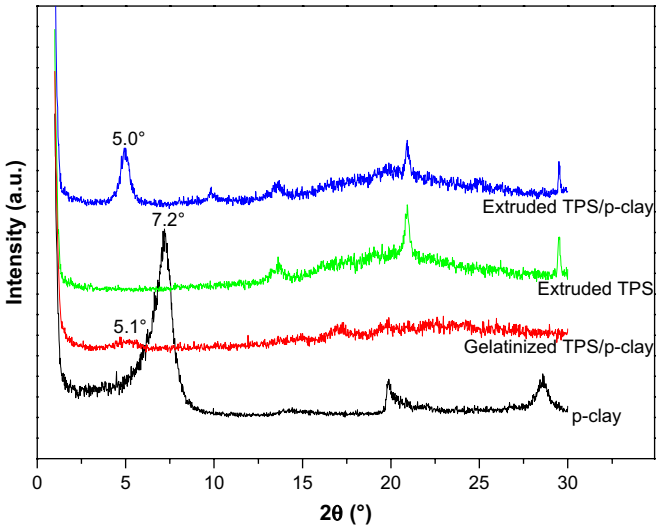

Fig. 7. XRDs of pristine clay (p-clay), extruded TPS and TPS/p-clay nanocomposites.

the free volume in starch. The diffraction parameters of native starch and TPS are summarized in Table 1.

Fig. 7 gives the XRDs of pristine clay, TPS and TPS/p-clay composites. Pristine clay shows a sharp (001) peak at $2\theta = 7.2^\circ$ corresponding to the spacing of 1.2 nm between individual clay layers, called *d*-spacing. The (001) peak becomes sharper and stronger after melt extrusion, the reason is that the clays in composites undergo an orientation process during hot pressing for specimen preparation which results in the sharper peak (001) than the gelatinized starch without hot pressing. The (001) peak shifts to 5.1° (*d*-spacing = 1.7 nm) after gelatinization with glycerol, however, it only shows a small change to 5.0° (*d*-spacing = 1.8 nm) after extrusion with starch indicating a small increase in clay spacing. Generally, the *d*-spacing of clay will be enlarged after melt compounding with a polymer, but it is worthy to note that the difference in (001) diffraction positions between p-clay and starch/p-clay

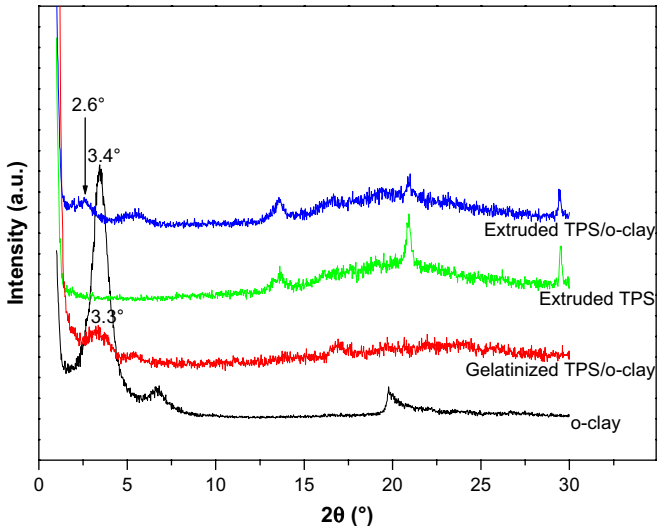

Fig. 8. XRDs of organically modified clay (o-clay), extruded TPS and TPS/o-clay nanocomposites.

is not significant. As we know, starch is a linear molecule consisting of ring-like monomer with size of about 0.55 nm, and generally starch has much higher molecular weight than common polymers [16]. It was reported that the molecular weight of corn starch with high content of amylose is about 2.4×10^7 g/mol resulting in a large gyration radius (163 nm) [22]. On the other hand, large numbers of inter- and intra-hydrogen bonds formed among and within starch molecules reduce the molecular mobility which furthermore hinders the starch intercalation. As shown in Fig. 7, glycerol expands the *d*-spacing of pristine clay to 1.7 nm after gelatinization and the valid spacing between nano clay layers is only 0.7 nm considering the thickness of a single nano clay layer is about 1 nm, thus it could be concluded that the increase in *d*-spacing of pristine clay after melt extrusion with starch is mostly due to the intercalation of glycerol but not starch molecules as indicated by the quite small shift to low angle of (001) peak of p-clay since the *d*-spacing is relatively narrow for sufficient starch intercalation due to its large molecular size.

The XRDs of starch/o-clay nanocomposites are shown in Fig. 8 and the crystalline parameters of TPS/o-clay are also summarized in Table 1. As seen, TPS/o-clay nanocomposites exhibit a Va-type crystalline structure similar to the TPS but the intensity of diffraction peaks of TPS decreased after compounded with o-clay due to the hindrance effect of nano clay layers. The organically modified clay shows a sharp (001) diffraction at $2\theta = 3.4^\circ$ corresponding to a *d*-spacing of 2.6 nm. After gelatinized with glycerol and starch, the peak shows a small shift to $2\theta = 3.3^\circ$ indicating that glycerol further expands the *d*-spacing of o-clay, however, starch molecules intercalated into clay galleries after melt compounding and expanded the spacing of clay as indicated by the (001) peak of the o-clay appearing at $2\theta = 2.6^\circ$ (*d*-spacing = 3.4 nm) which is not only because of the higher *d*-spacing of organically modified clay but also due to the improved interface compatibility between starch and o-clay since the intercalation

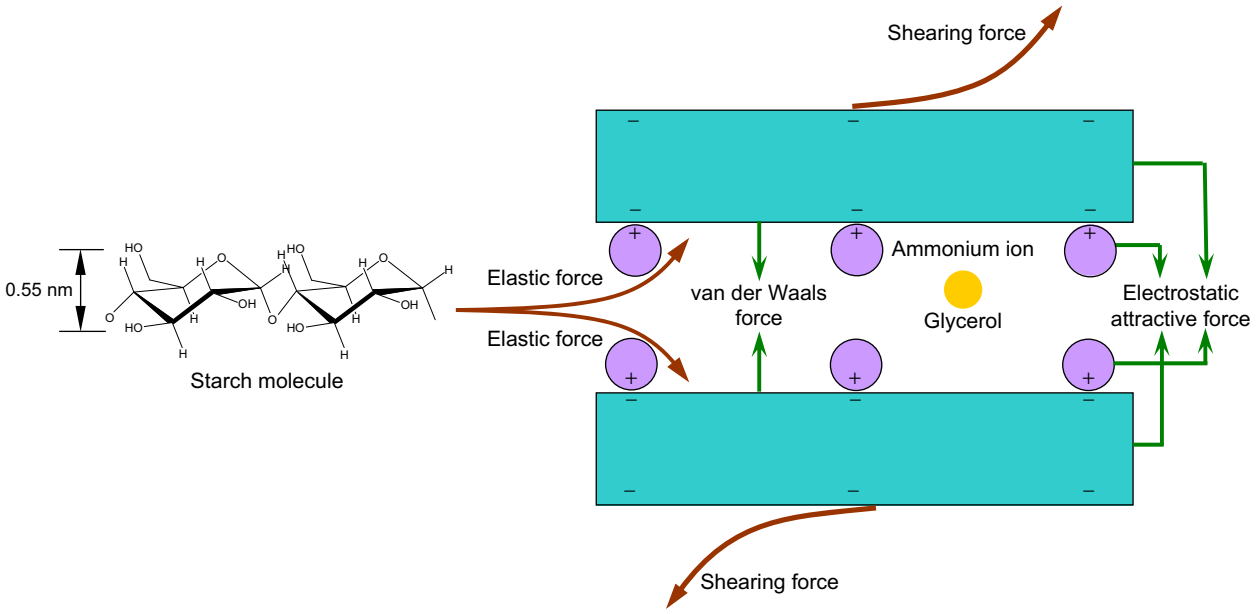

Fig. 9. Schematic depicting the intercalation process between starch and organically modified clay.

of glycerol into clay might change the hydrophobicity of clay surface to some extent.

The main force components operating on a pair of adjacent clay layers are illustrated in Fig. 9. The sum of van der Waals force and electrostatic attractive force against clay exfoliation, while the shearing force and elastic force arising due to starch molecular intercalation favor clay exfoliation. Clay exfoliation in polymer matrix by melt compounding mainly depends on two processes, namely, polymer chain intercalation into clay galleries, and nano clay layers exfoliation under shearing force. Both molecular weight and polar interactions between the clay and the polymer could influence polymer intercalation [23]. The organically modified clay provides much greater *d*-spacing than the size of starch monomer facilitating starch molecular intercalation. Both the larger *d*-spacing and modification by glycerol contribute to starch intercalation/exfoliation, however, the low compatibility between hydrophobic organically modified clay and hydrophilic starch reduce the diffusing of starch molecules into clay galleries and lower the effect of shearing force. Hydrophobic organically modified clay is favourable to compound with most of synthesized polymers, but it is immiscible with hydrophilic biomacromolecules such as starch. Therefore, it could be concluded that using hydrophilic modified clays could be a promising way to further improve clay exfoliation.

4. Conclusion

Biodegradable TPS/clay nanocomposites were prepared by melt processing using a pristine clay and an organically modified clay. The initial and maximum decomposition temperatures of TPS were enhanced with incorporation of pristine clay, but the organically modified clay only improved the initial decomposition temperature of TPS. Homogenous and transparent TPS/clay films were fabricated which are important for application as packing materials. B-type crystalline structure of native starch was observed and it transformed into Va-type structure after melt extrusion. The intercalation of starch into clay galleries was discussed from a viewpoint of molecular structure. The compatibility between starch and clay plays an important role for starch intercalation, but a large *d*-spacing is primarily necessary for starch intercalation considering the high molecular weight of starch and ring-like starch molecular monomer.

Acknowledgments

Jim Chambers and Associates in New South Wales, Australia was gratefully acknowledged for supply of both pristine clay and Cloisite 93A nano clay. Professor Yiu-Wing Mai at the Centre for Advanced Materials Technology (CAMT), the University of Sydney, is greatly acknowledged.

References

[1] Gross RA, Kalra B. Science 2002;297:803–7.
[2] Jiang L, Wolcott MP, Zhang J. Biomacromolecules 2006;7:199–207.
[3] Ray SS, Okamoto M. Prog Polym Sci 2003;28:1539–641.
[4] Lenz RW, Marchessault RH. Biomacromolecules 2005;6:1–8.
[5] Lörcks J. Polym Degrad Stab 1998;59:245–9.
[6] Kojima Y, Usuki A, Kawasumi M, Okada A, Kurauchi T, Kamigaito O. J Polym Sci Part A Polym Chem 1993;31:983–6.
[7] Kojima Y, Usuki A, Kawasumi M, Okada A, Kurauchi T, Kamigaito O, et al. J Polym Sci Part B Polym Phys 1994;32:625–30.
[8] Park HM, Li X, Jin CZ, Park CY, Cho WJ, Ha CS. Macromol Mater Eng 2002;287:553–8.
[9] Park HM, Lee WK, Park CY, Cho WJ, Ha CS. J Mater Sci 2003;38:909–15.
[10] Wilhelm HM, Sierakowski MR, Souza GP, Wypych F. Carbohydr Polym 2003;52:101–10.
[11] Huang MF, Yu JG, Ma XF. Polymer 2004;45:7017–23.

[12] Chiou BS, Yee E, Glenn GM, Orts WJ. Carbohydr Polym 2005;59: 467–75.
[13] Avella M, Vlieger JJD, Errico ME, Fischer S, Vacca P, Volpe MG. Food Chem 2005;93:467–74.
[14] Chen B, Evans JRG. Carbohydr Polym 2005;61:455–63.
[15] Qiao X, Jiang W, Sun K. Starch 2005;57:581–6.
[16] Buléon A, Colonna P, Planchot V, Ball S. Int J Biol Macromol 1998;23: 85–112.
[17] Romero-Bastida CA, Bello-Pérez LA, García MA, Martino MN, Solorza-Feia J, Zaritzky NE. Carbohydr Polym 2005;60:235–44.
[18] National Starch and Chemical Company. Food products division. Technical service bulletin. HYLON VII.
[19] Xie W, Gao Z, Pan WP, Hunter D, Singh A, Vaia R. Chem Mater 2001; 13:2979–90.
[20] Tester RF, Karkalas J, Qi X. J Cereal Sci 2004;39:151–65.
[21] van Soest JJG, Hulleman SHD, de Wit D, Vliegenthart JFG. Ind Crop Prod 1996;5:11–22.
[22] Bello-Pérez LA, Roger P, Baud B, Colonna P. J Cereal Sci 1998;27: 267–78.
[23] Vaia RA, Giannelis EP. Macromolecules 1997;30:8000–9.